The spatial tuning of color and luminance peripheral vision measured with notch filtered noise masking

Kathy T. Mullen *, M. Angeles Losada

Department of Ophthalmology, McGill Vision Research, McGill University, 687 Pine Avenue West, Montreal, H3A 1A1, Canada

Abstract

We have measured the spatial bandwidths of the bandpass red-green chromatic and luminance mechanisms at four locations in the nasal visual field (0, 10, 20 and 30°) using a method of notch filtered noise masking which effectively removes the artifact of off-frequency looking for our stimuli. Detection thresholds were measured for luminance or isoluminant red-green Gaussian enveloped test gratings of 0.5 cpd embedded in 1/f noise. Firstly, thresholds were obtained as a function of increasing noise spectral density and were fitted using a standard noise masking model. These results support the existence across the visual field of independent, red-green chromatic and luminance mechanisms with similar sampling efficiencies. Secondly, we measured thresholds in notch filtered noise as a function of notch width and derived the spatial bandwidth of the detection mechanism. We find both color and luminance mechanisms have similar bandwidths which remain virtually constant across eccentricity. These results indicate strong overall similarities between the early processing of color and luminance vision, and lend support to the role of color as an 'intrinsic image' in spatial vision. The results are discussed in the light of the anchored channel and shifting channel models of peripheral contrast sensitivity and pattern detection. © 1998 Elsevier Science Ltd. All rights reserved.

Keywords: Color vision; Noise masking; Spatial tuning; Isoluminance

1. Introduction

In luminance vision, the existence of visual channels acting in parallel, each selectively sensitive to a limited range of spatial frequencies is widely accepted. The shape and spatial tuning of these channels has been estimated using a variety of means: suprathreshold masking with narrowband stimuli (Legge & Foley, 1980; Wilson, McFarlane & Phillips, 1983) or with visual noise (Carter & Henning, 1971; Stromeyer & Julesz, 1972; Henning, Hertz & Hinton, 1981), sub-threshold summation (Sachs Nachmias & Robson, 1971), and spatial adaptation (Blakemore & Campbell, 1969). Although the estimates of the bandwidths may vary, these studies are in overall agreement and reveal luminance channels with bandpass characteristics at detection threshold. More recent psychophysical results based on narrowband masking (Bradley, Switkes & De Valois, 1988; Humanski & Wilson, 1992, 1993; Pandey

& Vimal, 1993; Losada & Mullen, 1994), noise masking (Losada & Mullen, 1995), and spatial adaptation (Bradley, Switkes & De Valois, 1988) indicate that color vision, like luminance vision, encodes the visual scene into a range of spatial scales by bandpass filtering. Thus although, color vision has overall spatial lowpass contrast sensitivity characteristics, this belies the bandpass nature of the underlying spatial chromatic channels. The chromatic masking studies in particular suggest strong overall similarities in the early processing of color and luminance vision, as both narrowband and notch filtered noise masking reveal that chromatic and luminance channels have very similar bandwidths over a range of spatial frequencies (Losada & Mullen, 1994, 1995).

The aims of this paper are two-fold. Firstly, we aim to measure the spatial tuning of the luminance visual channels for parafovea and eccentric vision. Secondly, we wish to continue the investigation of the underlying spatial tuning of color vision by comparing color and luminance channel bandwidths across the visual field. We do this using a method of notch filtered noise

---

* Corresponding author. Tel.: + 1 514 8421231 ext.4757; fax: + 1 514 8431691; e-mail: kmullen@violet.vision.mcgill.ca

masking, which has the key advantage of avoiding contamination of the measurements from off-frequency looking.

Curiously, there have been very few reports on the variation of channel bandwidths with eccentricity. Sharpe & Tolhurst (1973) used spatial frequency adaptation to reveal the presence of bandpass mechanisms for a 2 cpd test at 10° eccentricity, but made no quantitative comparisons with foveal data. There are several different models for the loss of contrast sensitivity with eccentricity (Garcia-Perez & Sierra-Vazquez, 1996). The loss in contrast sensitivity may be attributed simply to a change in channel gain, termed an anchored channel model (Watson, 1982), or to changes in channel gain combined with a shift in peak spatial frequency, termed a shifting channel model (Watson, 1983; Swanson & Wilson, 1985; Wilson, 1991). Neither of these models assume any a priori change in channel bandwidth with eccentricity, however the two models have different implications for our measurements. The anchored channel model predicts that channel bandwidth at any fixed spatial frequency will remain unchanged with eccentricity. Predictions from the shifting channel model require further assumptions about the dependence of channel bandwidth on spatial frequency. In the fovea, narrowband masking studies suggests that channel bandwidth (in octaves) narrows by approximately one octave across the whole spatial frequency range (0.5–16 cpd) (Wilson, McFarlane & Phillips, 1983; Wilson, 1991). In this case the shifting channel model would predict a narrowing of bandwidth with eccentricity for a fixed spatial frequency, since at greater eccentricities a fixed frequency will activate relatively higher spatial frequency channels within the overall population. In this paper we measure channel bandwidth with a fixed spatial frequency test stimulus in order to shed light on the relevance of these two models for the loss in contrast sensitivity with eccentricity. Furthermore, a knowledge of the dependence of channel bandwidths on eccentricity is required when modeling the deterioration with eccentricity in performance on spatial tasks such as vernier alignment, localization, or pattern discrimination (Wilson, 1991).

As for color vision, the loss in red–green contrast sensitivity with eccentricity is much steeper than for luminance vision reflecting the role of color as a foveal specialization (Mullen, 1991; Mullen & Kingdom, 1996), and nothing is known about the relative changes with eccentricity in the chromatic spatial channels subserving detection. Thus our aim is to find whether the similarity of luminance and chromatic spatial bandwidths already found in the fovea can be extended to the paracentral and peripheral regions of the visual field.

In the investigation we use symmetric notched noise which is obtained by adding two noise bands with symmetric cut-offs above and below the test spatial frequency. In the presence of multiple detection mechanisms, this method offers advantages over the use of separate high and lowpass noise masks, and to the use of narrowband masks. While many previous masking studies have assumed that a single mechanism determines detection threshold of the test stimulus (Stromeyer & Julesz, 1972; Legge & Foley, 1980; De Valois & Switkes, 1983; Switkes, Bradley & De Valois, 1988), a more realistic model requires the supposition of multiple mechanisms, with peaks spanning the spatial frequency range (Carter & Henning, 1971; Wilson, McFarlane & Phillips, 1983; Foley & Yang, 1991; Foley & Boynton, 1992). The assumption of multiple mechanisms complicates the determination of the spatial tuning of the detection mechanisms. In particular, in the presence of high contrast masking stimuli, the detection of the test may be subserved by mechanisms with a center frequency shifted away from the test frequency, thus optimizing the detection threshold. This effect was first found in auditory masking and termed off-frequency-listening (Patterson, 1976) and the corresponding effect in vision has been termed off-frequency looking (Pelli, 1980). Evidence for multiple mechanisms detecting the test has been found in spatial masking using both noise (Pelli, 1980; Blake & Holopigian, 1985; Perkins & Landy, 1991; Losada & Mullen, 1995) and narrowband masks (Wilson, McFarlane & Phillips, 1983; Foley & Yang, 1991). Unless taken into account, off-frequency looking will narrow the estimates of the bandwidths of the detection mechanisms, and this effect was demonstrated for both luminance and chromatic stimuli for high power noise masks (Losada & Mullen, 1995). Off-frequency looking can be prevented by using notch filtered noise (Patterson, 1976; Patterson & Nimmo-Smith, 1980; Blake & Holopigian, 1985; Patterson & Moore, 1986; Losada & Mullen, 1995). Losada & Mullen (1995) used this method in the fovea and reported that color and luminance vision have similar bandwidths which remain approximately constant over the range of spatial frequencies tested. In this paper we extend these results to examine the bandwidths of the color and luminance mechanisms across the visual field.

We have measured noise masking over a range of eccentricities for color and luminance contrast sensitivity. We find that for a fixed spatial frequency bandwidths remain constant from 0–30°, and that color and luminance bandwidths are similar. Thus these results lend further support to the idea that the color and luminance systems have similar spatial organizations.

2. Methods

2.1. Stimuli and apparatus

The stimulus generation and apparatus have been described in detail elsewhere (Mullen, 1985; Mullen & Boulton, 1992). Stimuli were produced by displaying two luminance modulated gratings, each on a Joyce (DM2) display screens with white P4 phosphors which were viewed through narrowband interference filters (Melles Griot) with centre wavelengths of 527 and 606 nm, respectively, and full bandwidths at half height of 21–22 nm. The two monochromatic gratings were combined spatially 180° out of phase by a beam splitter to produce a chromatic stimulus, or in phase for a luminance stimulus of the same mean luminance and chromaticity. Longitudinal and transverse chromatic aberrations were corrected by Mullen (1985). A bite bar was used to align the observer's head. Viewing was monocular and with a natural pupil. Stimuli had a mean luminance of 22 cpd m^{-2} and were centrally fixated using a small fixation spot. All stimuli were generated using a VSG2/1 waveform generator (Cambridge Research Systems) with 14 bit analogue output DACs. The 12 bit LUTs were mapped on to the 14 bit DAC values. Linearization of the phosphors of the display monitors was done in hardware within the DM2 monitors, so no software gamma correction was required and the loss of dynamic range usually incurred in this process was avoided. Linearization was verified using a UDT optometer (model S370) fitted with a photometer head (# 265) and any small imperfections were removed in software using corrections in the LUTs. The goodness-of-fits of the look-up-tables to the light output of the monitors produced a contrast error for the displayed stimuli of within 0.017 log units.

Test stimuli were horizontal Gaussian enveloped red-green isoluminant gratings, or isochromatic luminance gratings with a spatial frequency of 0.5 cpd. Noise masking stimuli were static luminance or chromaticity modulations displayed horizontally. All the chromatic and luminance noise masks were lowpassed with a cut-off in the fovea of 5.7 and 4 cpd for all non-foveal presentations, in order to reduce any luminance artifacts in the chromatic noise arising from chromatic aberration or an inaccurate isoluminant point. Uncorrelated one-dimensional random noise distributions were digitally generated and filtered in the Fourier domain with lowpass, highpass, bandpass, and notched filters. Test and mask were Gaussian enveloped along the axis of modulation. The Gaussian width at 1/e of its maximum height was three test cycles (6°). On the horizontal axis, test and mask were sharply truncated at a bar length of four cycles of the test stimulus (8°).

Contrast of the two luminance component gratings was defined by:

$$C = (I_{max} - I_{min})/(I_{max} + I_{min}) \tag{1}$$

where I_{max} and I_{min} are the peak and trough luminance values of the monochromatic grating, respectively. To determine isoluminance, the mean luminances of the two component gratings were varied while their contrasts were held constant. The contrasts of both the isoluminant chromatic grating and the homochromatic luminance grating are defined as the contrast of the component gratings (C).

Isoluminance of the two colors was measured using a minimum motion method (Moreland, 1982; Cavanagh, Tyler & Favreau, 1984; Mullen & Boulton, 1992). Subjects found the point at which the perceived drift rate of a (4 Hz) sinewave grating reached a minimum, by varying the ratio of the red-green mean luminance in the stimulus with a method of adjustment. This was repeated at least ten times and an average obtained. A representation of the chromatic and luminance stimuli in a cone contrast space can be found in Mullen & Losada (1994).

For reasons discussed in Section 1, we have used a fixed spatial frequency to measure bandwidths across the visual field, rather than a stimulus whose spatial frequency is scaled with eccentricity. This choice is also convenient since the notch noise is restricted by a lower spatial frequency limit (dependent on screen size and spatial frequency sampling limits), making it impractical to apply noise masks to very low spatial frequency test stimuli, as required for a test stimulus that is rescaled at greater eccentricities. The choice of a relatively low test spatial frequency (0.5 cpd) has the advantage of reducing the possibility of chromatic aberrations in the fovea or periphery.

2.2. Psychophysical methods

Thresholds were measured using a standard two-alternative forced choice staircase procedure. A noise mask appeared in both of the two time intervals, and was accompanied by the test stimulus in one interval. Test and mask stimuli was superimposed. The noise mask was different in each interval and a new pair was used for every trial. The static stimulus was presented with a temporal Gaussian envelope with a spread at 1/e of 125 ms (corresponding to a Fourier bandwidth of 2.5 Hz). The stimulus was stationary, and the phase of its presentation within the envelope was randomly varied between each interval. The subject indicated by pressing a button in which interval the test stimulus had appeared, and feedback was given after each trial. The initial step size of the staircase was 3 dB, but this was reduced to 1 dB after the first two reversals. The staircase procedure was terminated after eight reversals in the contrast presented, and the threshold was determined as the mean of the contrasts of the last five

reversals. Each plotted threshold represents the mean of at least three and up to five measured thresholds. Results were obtained on two subjects (KTM, MAL) with normal color vision measured on the standard tests (Farnsworth Munsell 100 Hue Test; The City University Colour Vision Test).

2.3. Digital generation of noise

This has been described fully elsewhere (Losada & Mullen, 1995). We use noise whose power density is constant when spatial frequency is measured in octaves rather than in linear units. The choice of a power density that varies as 1/f is supported by psychophysical results which suggest that, at least over the low-mid spatial frequency range (0.5–4 cpd), the spatial visual channels are similar in their octave bandwidths rather than in linear bandwidths (Henning, Hertz & Hinton, 1981; Henning, 1988; Rovamo, Franssila & Nasanen, 1992; Losada & Mullen, 1995; Blackwell, 1998). In this case each spatial frequency channel passes constant power from the 1/f noise. However, the use of 1/f rather than white noise has no practical consequences for the measurements reported in this paper since a fixed test spatial frequency is used. The notch band and lowpass filtering was done using step functions smoothed by a Hanning window to reduce ringing and to remove noise from the 'floor' of the stopband (Losada & Mullen, 1995).

2.4. A power spectrum model using a 1/f noise power density

To obtain the mechanism tuning functions it is necessary to postulate a model with several assumptions. We use a similar model to that in auditory psychophysics (Patterson & Moore, 1986) which has also been applied in visual masking (Pelli, 1980; Henning Hertz & Hinton, 1981). The noise is represented by its power density function ($\rho(f)$) and the mechanism by its transfer function ($H(f)$). Thus, the general masking equation is:

$$P_t = P_0 + K \int_{-\infty}^{+\infty} \rho(f)|H(f)|^2 \, df \qquad (2)$$

where P_t, the power of the test at threshold, is proportional to c^2. P_0 is the power of the internal noise which limits mechanism performance in the absence of external noise (Burgess, Wagner, Jennings & Barlow, 1981; Legge, Kersten & Burgess, 1987). At power densities which are high compared to the internal noise, Eq. (2) indicates that test power at threshold is proportional (K) to the power of the noise transmitted by the filter (i.e. filter's signal-to-noise ratio at threshold is constant).

Eq. (2) can be solved by choosing a masking stimulus whose power density simplifies the integral, such as lowpass, highpass, bandpass or notch noise. If noise power density is constant when varying noise bandwidth ($\rho(f) = \rho_0$), Eq. (2) yields:

$$P_t = P_0 + K\rho_0 \int_B |H(f)|^2 \, df \qquad (3)$$

where the limits of the integral are determined by B, representing the band of the noise filter in the frequency domain. Thus, the total power of the noise band changes for different filter sizes reflecting the integral of the filter shape over the region of overlap. The notch filters used for the noise were also defined on an octave scale.

2.5. Control experiments for the use of noise masks

Control experiments assess the noise masks in three respects:

1. As already mentioned, the frequency content of chromatic and luminance noise was lowpassed to below 5.7 cpd in the fovea and below 4 cpd for all eccentric presentations in order to limit possible artifacts in the chromatic noise from chromatic aberration, or from an inaccurate isoluminant point. Results for foveal stimuli have shown that thresholds for the detection of chromatic test gratings are unaffected (or slightly facilitated) by luminance noise at low-medium noise spectral densities (Gegenfurtner & Kiper, 1992; Losada & Mullen, 1995; Sankeralli & Mullen, 1997). Thus, any artifactual luminance contrast arising in the chromatic noise mask is unlikely to affect chromatic detection thresholds. Nevertheless, since aberrations are greatest in the periphery, we also performed control experiments measuring the detection of luminance test gratings in the chromatic noise and vice versa, which are reported in Section 3.

2. Despite the lowpassing of the noise, it still provides a range of 3–3.5 octaves either side of the test spatial frequency. Removing this cut-off and allowing the noise to extend to the Nyquist frequency limit of the apparatus (22 cpd) has no effect on the masking of luminance test by luminance noise, or chromatic test by chromatic noise (Losada & Mullen, 1995). This confirms that the lowpass filtered noise can be considered uniform for the detection mechanism at 0.5 cpd.

3. In this study we use symmetrical notch filtered noise to investigate the bandwidths of the detection mechanisms. This assumes that the underlying chromatic and luminance detection mechanisms are bandpass in form, an assumption which is well accepted for luminance vision. For color vision, we have demonstrated bandpass filtering in the fovea using lowpass

Achromatic
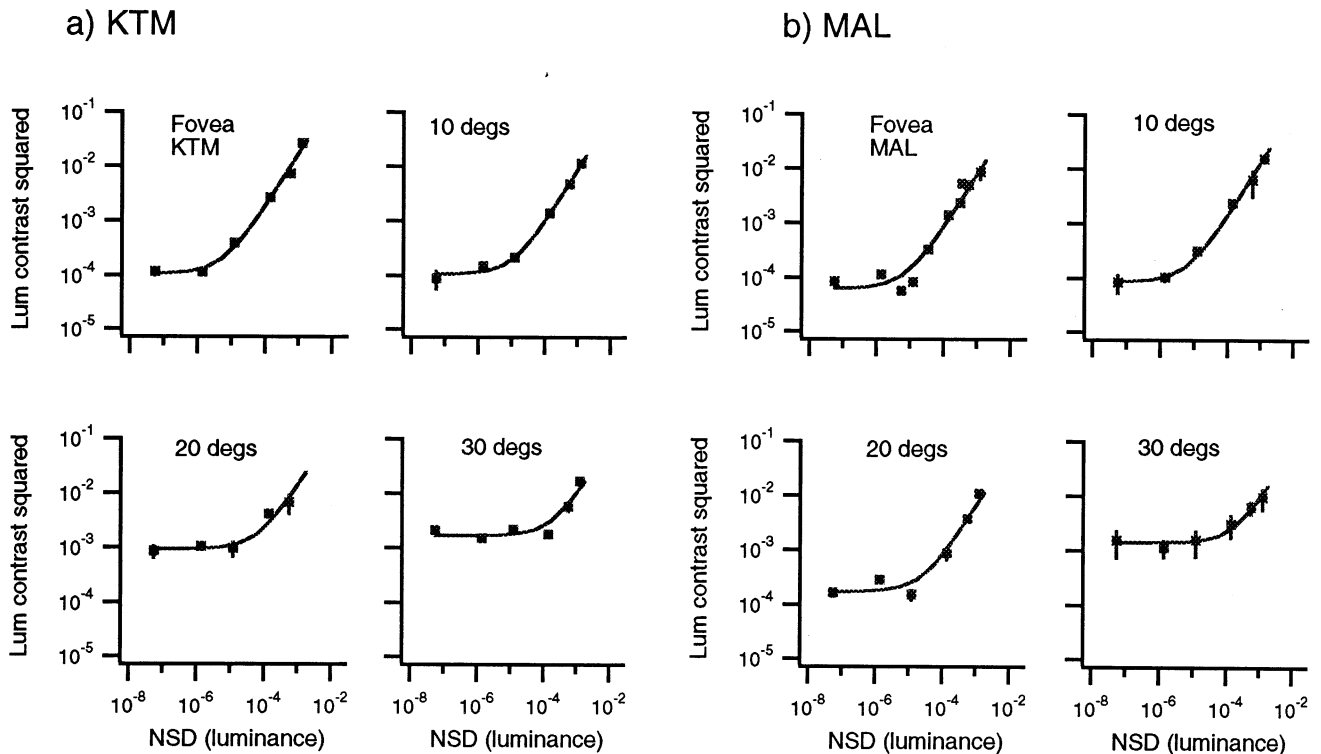
a) KTM

b) MAL

Fig. 1. Luminance contrast energy at threshold as a function of noise spectral density (NSD) plotted in (a) for KTM and (b) for MAL. The abscissa shows the power of the noise per octave and the ordinate shows the squared-test contrast threshold. Results for four retinal locations: fovea, 10, 20, and 30° into the nasal field. Error bars show ± 1 S.D. for each data point and are frequently smaller than the symbol size.

and highpass noise (Losada & Mullen 1995). We now assume that the bandpass shape of these filters is extended to paracentral and peripheral vision.

3. Results

3.1. Thresholds versus noise spectral density

Figs. 1 and 2 show results for thresholds measured in broadband noise of varying noise power densities. Four different eccentricities (0, 10, 20, and 30°) were sampled and the noise masking functions were obtained for luminance test stimuli in luminance noise (Fig. 1) and color test stimuli in color noise (Fig. 2) for two subjects. Overall, contrast sensitivity declines with eccentricity more rapidly for red–green chromatic stimuli than for luminance stimuli (Mullen, 1991; Mullen & Kingdom, 1996) hence we were unable to obtain chromatic thresholds at eccentricities greater than 10°. The contrast energy of the test stimulus at threshold (the square of threshold contrast) is plotted as a function of the noise power density on log–log coordinates. Both chromatic and luminance functions at all eccentricities follow the same general form. Initially, at low power

densities, there is little masking, followed by a linear rise with a slope near 1.

As already discussed, the effect of external noise is conveniently modeled by a system with an equivalent internal noise (P_0) and a limited sampling efficiency. The functions were fitted on log–log coordinates with a simplified version of Eq. (3)

$$P_t = P_0 + K*N \tag{4}$$

where N is the total noise power. Eq. (3) can be simplified as the test stimuli (and hence detection filters) are not varied in spatial frequency and N reflects only the variation in the applied noise power densities.

All calculated Q values for Figs. 1 and 2 were above 0.1, indicating a good fit of the model to the data (see later text for details). Thus these fits indicate that the model is a reasonable one to apply across the different conditions of color and eccentricity, supporting its use in the bandwidth analysis. Furthermore, both an indication of the internal noise and the sampling efficiency of eccentric color and luminance vision can be derived. The sampling efficiency is inversely proportional to the value of K (see Gegenfurtner & Kiper, 1992). Fitted values of K are plotted in Fig. 3 and provide a relative comparison of efficiencies across different conditions.
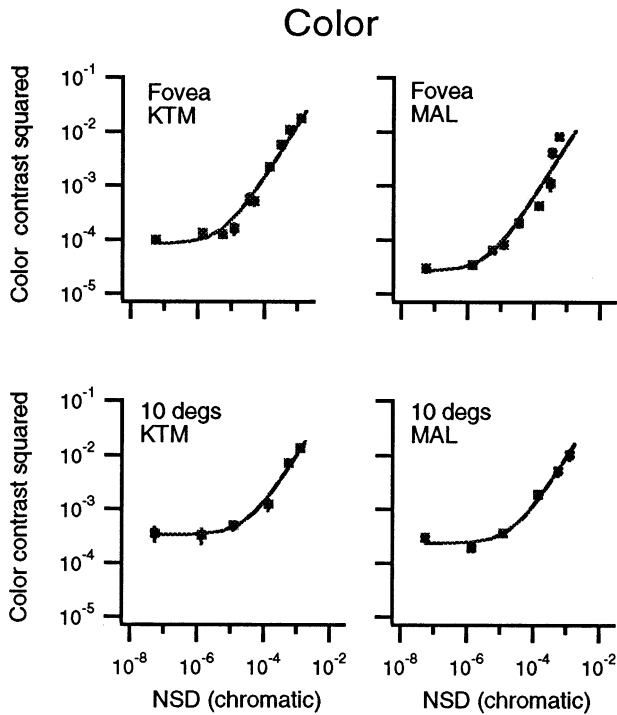
Color

Fig. 2. Isoluminant red-green contrast thresholds as a function of chromatic noise spectral density are shown on the left for KTM and on the right for MAL. Chromatic thresholds were not measurable beyond 10° of eccentricity. See legend of Fig. 1 for further details.

The efficiencies for color and luminance contrast are similar, supporting the conclusions of Gegenfurtner & Kiper (1992) for foveal vision. The dashed line shows a weighted linear regression applied to all the data combined across subject and color and luminance contrast. The fit shows a very shallow decline in K (increase in efficiency) indicating little dependence of efficiency on eccentricity. The fitted value of the internal noise (pro-
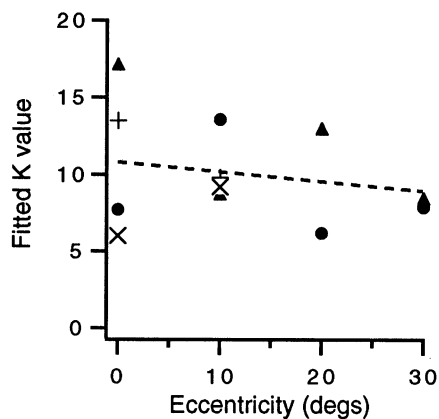

Fig. 3. Fitted K values (from Eq. (4)) are plotted as a function of eccentricity in degrees. Data for both subjects. Filled symbols for luminance contrast (triangles for KTM, circles for MAL) and crossed symbols for color contrast (+ KTM, × MAL). The fit is a weighted linear regression of all data combined. Note that K is inversely proportional to the sampling efficiency of vision.
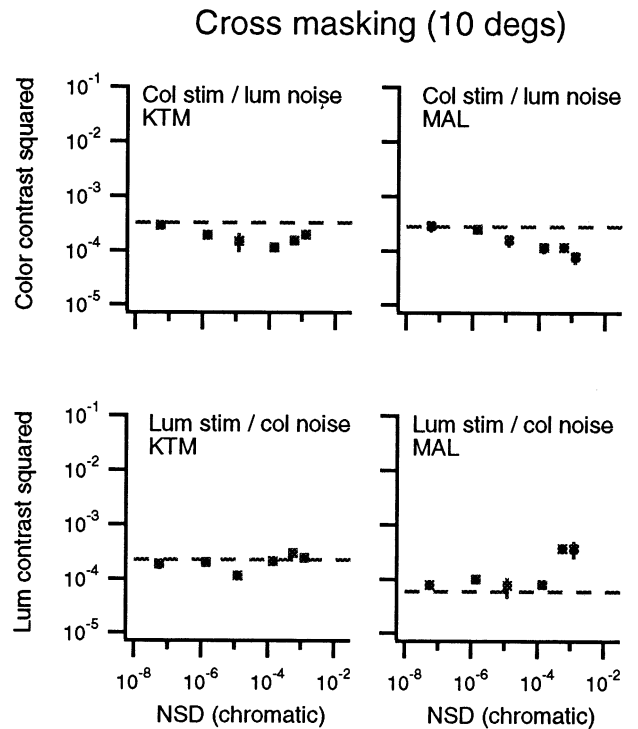
Cross masking (10 degs)

Fig. 4. Thresholds for the detection of chromatic gratings in the presence of luminance noise (top panels) and for luminance gratings in the presence of chromatic noise for (lower panels). Data on the left are for KTM, and on the right for MAL. The dashed line gives the no-noise thresholds. Measured at 10° in the nasal field. See legend of Fig. 1 for further details.

portional to P_0) is not shown, but in general increases with eccentricity, significantly more so for color vision, reflecting the steeper rise in thresholds already reported for red-green chromatic stimuli (Mullen, 1991; Mullen & Kingdom, 1996).

In Fig. 4, we report the effects of chromatic noise on luminance test stimuli, and luminance noise on chromatic tests. As this has been measured before in the fovea for our own experimental set-up (Losada & Mullen, 1995), and others (Gegenfurtner & Kiper, 1992; Sankeralli & Mullen, 1997), we have confined our measurement to 10° of eccentricity. For the detection of color contrast in the presence of luminance noise (top panels) there is no masking, but instead a small facilitation of threshold is found, consistent with previous reports (Losada & Mullen, 1995; Blackwell, 1998). For the detection of luminance contrast in color noise (lower panels), thresholds were unaffected (KTM) or slightly elevated at the highest noise spectral densities (MAL), resembling the results obtained in the fovea.

These experiments are useful controls for the presence of luminance artifacts in two respects. Firstly, as luminance noise is ineffective at elevating chromatic threshold, any luminance artifact in the chromatic noise will not affect our chromatic notch masking measurements. Secondly, as the chromatic noise produces none
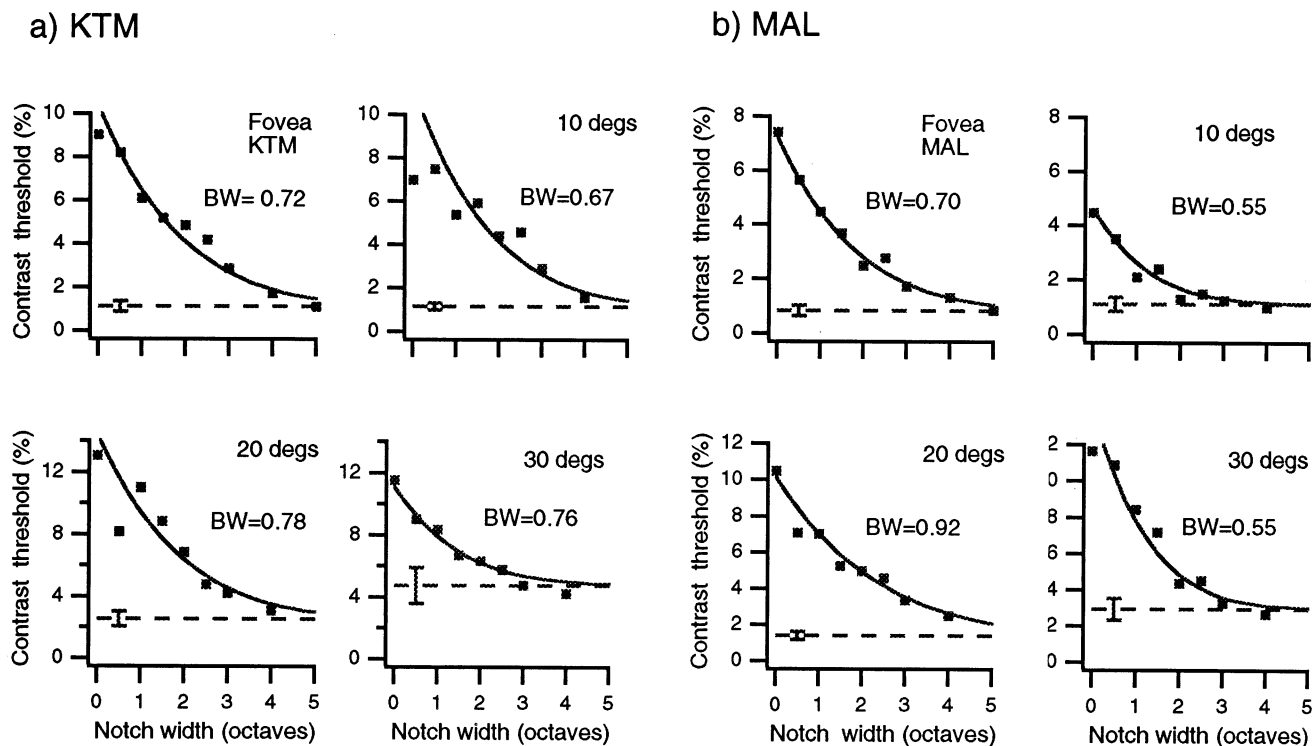
Achromatic

a) KTM

b) MAL

Fig. 5. Thresholds for luminance gratings in notched noise are shown in the left column for KTM and on the right for MAL, for the four retinal locations as marked. The abscissa shows the full notch width in octaves and the ordinate shows the masked contrast threshold (% contrast) on a linear scale. High noise spectral densities (NSD, power per octave) were used for the mask, selected from the functions of Figs. 1 and 2 for their greatest obtainable masking effect, and are as follows: fovea, 0.556×10^{-3} (KTM and MAL); 10°, 0.556×10^{-3} (KTM), 0.139×10^{-3} (MAL); 20 and 30°, 1.25×10^{-3} (KTM and MAL). Error bars show ± 1 S.D. averaged for each data set and converted to the linear units of the ordinate. Solid lines show the model fit to the data. The half-bandwidths at half height are marked on each curve. Most bandwidths were measured twice on each subject although only a single data set per subject is shown in this figure. (All data is used in Fig. 7). Q values indicating the goodness-of-fit of the data to the model are as follows: for KTM, $Q = 0.27$, < 0.001, 0.71, 0.98; for MAL, $Q = 0.58$, 0.83, 0.84, 0.13, given in order of panel presentation. Q values > 0.1 indicate a good fit of the model to the data.

or very little threshold elevation of the luminance tests, we can assume that it contains insignificant luminance artifact. Finally, the lack of interaction between test stimuli of one contrast type and noise of another contrast type suggests that independent color and luminance detection mechanisms exist in the periphery. This conclusion is supported in the fovea by the noise masking results cited above, and a by range of other methods (Cole, Hine & McIlhagga, 1993; Mullen Cropper & Losada, 1997). It is important for the interpretation of the bandwidth analysis since it confirms that the bandwidth measurements reported in the next section reflect the activities of separable color and luminance mechanisms.

3.2. Bandwidths for color and luminance mechanisms as a function of eccentricity

In this section we obtain thresholds in noise filtered with notches of different sizes (from 0.5 to 5 octaves) at

a given power density indicated in the legend. The same four eccentricities are tested. Fig. 5 shows the thresholds for achromatic gratings in achromatic notched noise, and Fig. 6 shows those for chromatic gratings in chromatic noise, for two subjects. In each figure, the abscissa shows notch width in octaves and the ordinate shows the masked contrast threshold (%) on a linear scale. The averaged standard deviation for each data set was calculated and is marked on each panel. All results have the same general form, showing a decrease in masking as the notch width is widened and the signal to noise ratio of the detection mechanism improves.

To obtain the bandwidths quantitatively we assume that the shape of the mechanisms can be described by two exponential functions joined back-to-back:

$$\exp\{+0.69(f - f_0)/B_1\} \quad \text{if } f < f_0 \qquad (5)$$

$$\exp\{-0.69(f - f_0)/B_u\} \quad \text{if } f \geq f_0 \qquad (6)$$

where f is the spatial frequency in octaves of the test frequency, f_0 is the central frequency of the mechanism, and B_l and B_u are the lower and upper sides of the bandwidths (defined at half height). The exponential shape has been used in auditory (Patterson & Moore, 1986), and visual noise masking (Pelli, 1980; Henning, Hertz & Hinton, 1981). The central frequency of the most sensitive mechanism is assumed to be equal to the test spatial frequency ($f_0 = 0$). We assume that the lower and upper sides of the mechanisms are equal: $B_l = B_u = B^1$. As we used a 1/f power density, the power of the test at threshold was given by Eq. (3) with f in octaves. The value of P_0 was fixed at the power of the test at threshold in the absence of external noise. The model was fitted to the data points for each set of results (solid lines) by varying the values of B and K. The bandwidths obtained are indicated beside each data plot. The Q values, providing a statistical measure of the goodness-of-fit of the model to the data, are given in the legend. A Q value gives the probability that the minimum χ^2 is as large as it is purely due to chance, even for a correct model. If the Q value is small, the

Fig. 7. Full bandwidth at half height (octaves) plotted as a function of eccentricity. Open symbols show data for luminance gratings and crossed symbols show data for chromatic red-green gratings. The solid line gives the weighted fit of a linear regression to all the data. Intercept = 1.34 octaves, slope = 0.012 octaves per degree. The dashed line gives the 5% confidence limit of the slope of the function and the error bar gives ± 1 S.D. of the intercept. The Q value (0.83) indicates that the fit is good.

residuals (O-E) are unlikely to be chance fluctuations, and the model is likely to be incorrect. A Q value greater than 0.1 is considered to indicate a good fit of the model to the data (Press, Teukolsky, Vetterling & Flannery, 1992). For the achromatic bandwidth measurements shown in Fig. 5, seven of the eight data sets display a good model fit to the data ($Q > 0.1$). For the chromatic measurements in Fig. 6, two of the four data sets show a good model fit.

Although only one set of data is shown for each subject, most of the notch masking functions were obtained twice on each subject in order to provide more reliable bandwidth estimates and an estimate of variability. Fig. 7 plots all the 18 bandwidth fits. Of the 18 estimates obtained in all, 14 displayed a good model fit with $Q > 0.1$. Full bandwidth ($2*B$) is plotted as a function of eccentricity. Individual results are given by the symbols. Luminance and color bandwidths averaged across subject and eccentricity are very similar: for color contrast, the averaged bandwidth is 1.5 ± 0.17 octaves, and for luminance contrast the bandwidth averaged across the same retinal locations (0 and 10°) is 1.4 ± 0.14 octaves. For luminance and color, there appears to be no discernible variation in bandwidth with eccentricity. The data on the figure have been fitted with a linear regression (solid line) which has an intercept of 1.34 ± 0.13 and a shallow slope (0.012 octave per degree) representing a change of 0.36 octaves across the eccentricity range of 30°. The dashed lines give the 5% confidence limits on the slope of the fit and the error bar gives ± 1 S.D. of the intercept. The data are quite tightly correlated ($r = 0.95$), and the fit is good ($Q = 0.83$). Furthermore, a slope of 0 falls within the
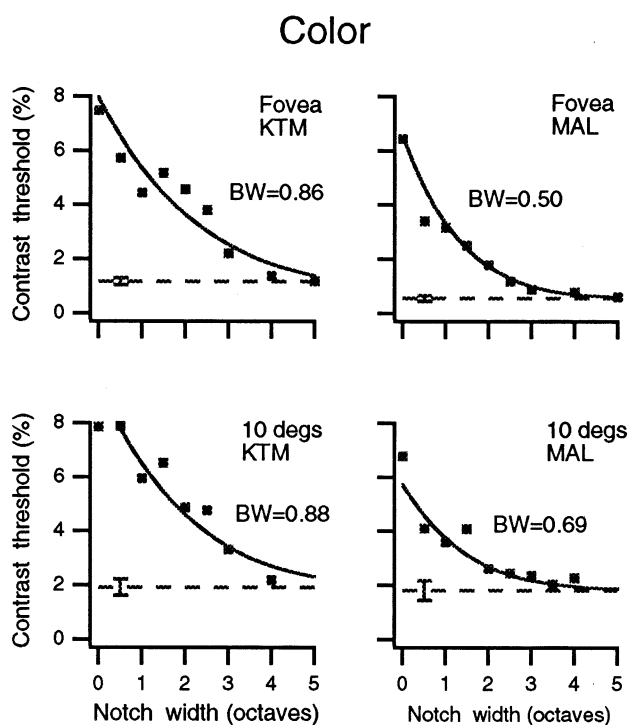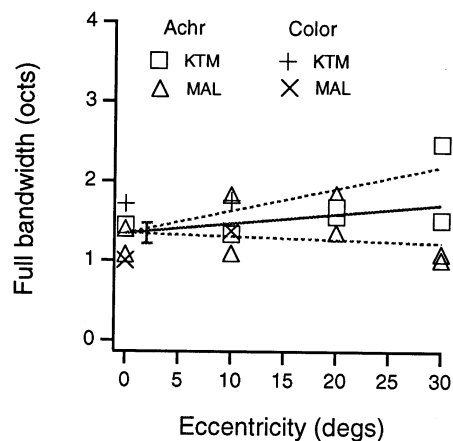
Color

Fig. 6. Thresholds for chromatic gratings in chromatic notched noise are shown in the left column for KTM and on the right for MAL. Noise spectral densities of the mask are as follows: fovea, 0.313×10^{-3} (KTM and MAL), 10°, 1.25×10^{-3} (KTM and MAL). Q values are as follows: for KTM, $Q = <0.01, <0.01$; for MAL, $Q = 0.74, 0.89$, given in order of panel presentation. Other conditions, as for Fig. 5.

---

[1] Note, however, that there is evidence for small asymmetries in the channel shapes (Henning, Hertz & Hinton, 1981; Henning, 1988; Losada & Mullen, 1995).

5% confidence limits of the data, and such a fit (of 0 slope) also provides an acceptable description of the data ($Q = 0.45$). These results show that bandwidth is effectively constant across eccentricity (at least up to 30°) for both color and luminance vision.

4. Discussion

Measurements of the bandwidths of the foveal spatial mechanisms using notch filtered noise masking have already been reported (Losada & Mullen, 1995), and in combination with our present results have an average bandwidth in the fovea of 1.3 octaves for both luminance and color. These are broadly compatible with the 1.5–2 octave bandwidth range reported in previous noise masking studies for test stimuli covering the range of 0.5–4 cpd (Stromeyer & Julesz, 1972; Pelli, 1980; Henning, Hertz & Hinton, 1981; Henning, 1988), and with the 1.75 bandwidth reported by Legge & Foley (1980) for a 2 cpd stimulus using narrowband masks. Wilson, McFarlane & Phillips (1983), using narrowband masks in experiments, have considered the effect of centre spatial frequency on bandwidth and report a narrowing of bandwidth with spatial frequency from around 2.5 octaves at spatial frequencies below 1 cpd to around 1.3 octaves at higher spatial frequencies (above 4 cpd). Thus when matched for spatial frequency, our bandwidths estimates are somewhat narrower than theirs.

For red-green chromatic mechanisms, noise masking and sinewave studies have shown that foveal color vision has spatially bandpass channels with similar shapes and bandwidths to those for luminance vision under equivalent conditions (Losada & Mullen, 1994, 1995), and the present results demonstrate that this similarity extends across the visual field. For blue-yellow chromatic mechanisms, Humanski & Wilson (1992, 1993) used a narrowband masking method and reported similar bandpass channels for blue-yellow color and luminance vision in the fovea. Thus our results add to a growing body of evidence which indicates strong overall similarities in the early processing of spatial information by color and luminance vision, since both process spatial patterns with similar early, narrowband spatial filtering.

Models for chromatic spatial pattern discrimination have not yet been extensively developed. Even though the shapes of the early chromatic and luminance mechanisms are similar, there may be other differences in the early filtering, for example in the numbers and sampling of the spatial filters. These might account for the poorer spatial frequency discrimination (by approximately double at low contrasts) that is found for color compared to luminance contrast (Webster, De Valois & Switkes, 1983). Spatial filtering models like those of Wilson (1991) could be used to explore these differences. There may also be differences in the subsequent stages of spatial processing, when the outputs of these early mechanisms are integrated to extract the salient and significant features of the image. For example, McIlhagga & Mullen (1996) report that performance on a contour integration task is around two times poorer at low contrasts for red-green chromatic stimuli compared to luminance stimuli which suggests that color vision may be poorer in integrating information across space and orientation. Overall, however, these differences in the performances on the color and luminance systems are rather small, and do not exclude color vision from having a primary role in spatial pattern discrimination and form detection.

As raised in Section 1, our results are relevant for current models of peripheral vision which are used to account for the loss in contrast sensitivity with eccentricity, and the decline in pattern discrimination and hyperacuities (Wilson, 1991). Our result, that bandwidth for a fixed spatial frequency is virtually constant with eccentricity, is somewhat at odds with the predictions of the shifting channel model, based on the results of Wilson, McFarlane & Phillips (1983) and Swanson & Wilson (1985). Wilson, McFarlane & Phillips (1983), using narrowband masking, have reported an overall decrease in bandwidth with spatial frequency (from 2.5 to 1.3 octaves in the range 0.5–4 cpd). Furthermore, Swanson & Wilson (1985) have suggested that a simple rescaling of the peak channel spatial frequencies to lower spatial frequencies provides a good account of peripheral masking data at 8° of eccentricity. Under this shifting channel model, we would have expected to find a narrowing in the tuning functions for a fixed spatial frequencies detected at greater eccentricities, since the test stimulus will probe channels with higher peak sensitivities relative to their position within the overall contrast sensitivity function. Swanson & Wilson (1985) scaled their spatial frequencies by a factor of 2 at 8°. Assuming that this scaling can be approximately linearly extrapolated with eccentricity, we would expect a factor close to 8 by 30°, rendering our spatial frequency the equivalent of 4 cpd in the fovea. From the data of Wilson, McFarlane & Phillips (1983), we would expect a narrowing in bandwidth for detection of the 0.5 cpd test stimulus from about 2.5 to 1.3 octaves over our eccentricity range. Such a change is outside the confidence limits of our data, and if anything our data suggest instead a slight broadening of spatial tuning.

Various possible explanations for these differences can be considered. Firstly, an anchored channel model rather than a shifting channel one, may best apply to peripheral contrast sensitivity. This model assumes that the channel detecting our 0.5 cpd test will undergo a loss in channel gain with eccentricity with no change in peak spatial frequency, and it predicts that the detec-

tion channel for a fixed spatial frequency remains constancy with eccentricity. This model is in keeping with our results which show that spatial mechanisms with particular centre frequency undergo no alterations in bandwidth.

A second possibility is that our results are specific to the spatial frequency used of 0.5 cpd, and that a different dependence of bandwidth on eccentricity would be found if higher spatial frequencies were investigated. We were constrained to choose a relatively low spatial frequency due to the dual considerations of chromatic aberration and the precipitous loss in red-green sensitivity away from the fovea. Only further investigation of the luminance mechanism can resolve this question.

Another interesting possibility is that the noise masking methods and narrowband masking produce different estimates of channel bandwidth across spatial frequency. This requires one to suppose that the narrowing of channel bandwidth reported by Wilson, McFarlane & Phillips (1983) and Wilson (1991) is not found in noise masking studies. No noise masking studies have yet explicitly measured the dependence of channel bandwidth on spatial frequency over a wide range of frequencies. The high and lowpass noise masking measurements of Henning, Hertz & Hinton (1981) and Henning (1988), suggest no narrowing of octave bandwidth with spatial frequency over the range 0.5–4 cpd. Other noise masking results imply indirectly that the channels are constant in octaves across spatial frequency over the same mid-low spatial frequency range. Losada & Mullen (1995) compared the effects of 1/f noise and flat white noise on the masking of a range of test spatial frequencies (0.5–4 cpd). The results showed that the effective masking of the 1/f noise was constant across spatial frequency, but masking increased when white noise was used. This results are consistent with channels whose bandwidths are constant in octaves. Under the model of Losada & Mullen, the one octave narrowing of bandwidth reported by Wilson, McFarlane & Phillips (1983) would have produced a 2-fold decline in effective masking across spatial frequency. The results of Rovamo, Franssila & Nasanen (1992) are also broadly consistent with channels that are constant in octaves. Although they too did not directly measure the effect of spatial frequency on visual channels, they measured white noise masking at different viewing distances which effectively provides 1/f noise. However, until notch filtered noise making is used to explicitly measure channel bandwidth across spatial frequency, the data of Wilson, McFarlane & Phillips (1983) remain the most detailed available.

In summary, it is commonly suggested that spatial tuning revealed by masking reflects receptive field structures at an early cortical stage (Graham, 1989; Wilson, 1991). In this case, the constancy of bandwidth across eccentricity for a fixed spatial frequency suggests that, across eccentricity, receptive fields of any one centre size maintain a constant structure in terms of the extent of the inhibitory and excitatory side-bands. Our data are thus compatible with the anchored channel model of peripheral contrast sensitivity. Providing future noise masking results support the narrowband masking data of Wilson, McFarlane & Phillips (1983) in showing a narrowing in channel bandwidth with spatial frequency, we can also conclude that our results are incompatible with the predictions of the shifting channel model and a narrowing of receptive field tuning with eccentricity.

Acknowledgements

References

Blackwell, K. T. (1998). The effect of white and filtered noise on contrast detection thresholds. *Vision Research*, *38*, 267–280.

Blake, R., & Holopigian, K. (1985). Orientation selectivity in cats and humans assessed by masking. *Vision Research*, *25*, 1459–1467.

Blakemore, C., & Campbell, F. W. (1969). On the existence of neurons in the human visual system selectively sensitive to the orientation and size of retinal images. *Journal of Physiology*, *203*, 237–260.

Bradley, A., Switkes, E., & De Valois, K. K. (1988). Orientation and spatial frequency selectivity of adaptation to color and luminance gratings. *Vision Research*, *28*, 841–856.

Burgess, A., Wagner, R. F., Jennings, R. J., & Barlow, H. B. (1981). Efficiency of human visual signal discrimination. *Science*, *214*, 93–94.

Carter, B. E., & Henning, G. B. (1971). The detection of gratings in narrow-band visual noise. *Journal of Physiology*, *219*, 355–365.

Cavanagh, P., Tyler, C. W., & Favreau, O. E. (1984). Perceived velocity of moving chromatic gratings. *Journal of the Optical Society of America A*, *1*, 893–899.

Cole, G. R., Hine, T., & McIlhagga, W. H. (1993). Detection mechanisms in L-, M-, and S-cone contrast space. *Journal of the Optical Society of America A*, *10*, 38–51.

De Valois, K. K., & Switkes, E. (1983). Simultaneous masking interactions between chromatic and luminance gratings. *Journal of the Optical Society of America A*, *73*, 11–18.

Foley, J. M., & Yang, Y. (1991). Forward pattern masking: effects of spatial frequency and contrast. *Journal of the Optical Society of America A*, *8*, 2026–2037.

Foley, J. M., & Boynton, G. M. (1992). Simultaneous pattern masking: mechanisms are revealed by threshold versus masker contrast functions and the direct measurement of masking sensitivity. *Investigative Ophthalmology and Visual Science Supplement*, *33*, 1256.

Garcia-Perez, M. A., & Sierra-Vazquez, V. (1996). Do channels shift their tuning towards lower spatial frequencies in the periphery? *Vision Research*, *36*, 3339–3372.

Gegenfurtner, K. R., & Kiper, D. C. (1992). Contrast detection in luminance and chromatic noise. *Journal of the Optical Society of America*, *9*, 1880–1888.

Graham, N. V. S (1989). *Visual Pattern Analyzers*. New York: Oxford University Press.

Henning, G. B., Hertz, B. G., & Hinton, J. L. (1981). Effects of different hypothetical detection mechanisms on the shape of spatial frequency filters inferred from masking experiments: I. noise masks. *Journal of the Optical Society of America*, 71, 574–581.

Henning, G. B (1988). Spatial-frequency tuning as a function of temporal frequency and stimulus motion. *Journal of the Optical Society of America A*, 5, 1362–1373.

Humanski, R. A., & Wilson, H. R. (1992). Spatial frequency mechanisms with short-wavelength-sensitive cone inputs. *Vision Research*, 32, 549–560.

Humanski, R. A., & Wilson, H. R. (1993). Spatial-frequency adaptation: evidence for a multiple channel model of short-wavelength-sensitive cone spatial vision. *Vision Research*, 33, 665–675.

Legge, G. E., & Foley, J. M. (1980). Contrast masking in human vision. *Journal of the Optical Society of America*, 70, 1458–1471.

Legge, G. E., Kersten, D., & Burgess, A. E. (1987). Contrast discrimination in noise. *Journal of the Optical Society of America A*, 4, 391–404.

Losada, M. A., & Mullen, K. T. (1994). The spatial tuning of chromatic mechanisms identified by simultaneous masking. *Vision Research*, 34, 331–341.

Losada, M. A., & Mullen, K. T. (1995). Color and luminance spatial tuning estimated by noise masking in the absence of off-frequency looking. *Journal of the Optical Society of America A*, 12, 250–260.

McIlhagga, W. H., & Mullen, K. T. (1996). Contour integration with color and luminance contrast. *Vision Research*, 36, 1265–1279.

Moreland, J. D. (1982). Spectral sensitivity measured by motion photometry. *Documenta Ophthalmologica Proceedings Series*, 33, 61–66.

Mullen, K. T. (1985). The contrast sensitivity of human color vision to red-green and blue-yellow chromatic gratings. *Journal of Physiology*, 359, 381–409.

Mullen, K. T. (1991). Colour vision as a post receptoral specialization of the central visual field. *Vision Research*, 31, 119–130.

Mullen, K. T., & Boulton, J. C. (1992). Absence of smooth motion perception in color vision. *Vision Research*, 32, 483–488.

Mullen, K. T., & Losada, M. A. (1994). Evidence for separate pathways for color and luminance detection mechanisms. *Journal of the Optical Society of America A*, 11, 3136–3151.

Mullen, K. T., Cropper, S. J., & Losada, M. A. (1997). Absence of linear subthreshold summation between red-green and luminance mechanisms over a wide range of spatiotemporal conditions. *Vision Research*, 37, 1167–1175.

Mullen, K. T., & Kingdom, F. A. (1996). Losses in peripheral color sensitivity predicted from 'hit and miss' post-receptoral cone connections. *Vision Research*, 36, 1995–2000.

Pandey, R., & Vimal, R. L. P. (1993). Threshold elevation curves for the red-green channel estimated by oblique masking. *Investigative Ophthalmology and Visual Science Supplement*, 34, 751.

Patterson, R. D. (1976). Auditory filter shapes derived with noise stimuli. *Journal of Acoustic Society of America*, 59, 640–654.

Patterson, R. D., & Nimmo-Smith, I. (1980). Off-frequency listening and the auditory filter asymmetry. *Jouranl of Acoustic Society of America*, 67, 229–241.

Patterson, R. D., & Moore, B. C. J. (1986). Auditory filters and excitation patterns as representations of frequency resolution. In B. C. J. Moore, *Frequency selectivity in hearing*. London: Academic Press, 123–177.

Pelli, D. G. (1980). Channel properties revealed by noise masking. *Investigative Ophthalmology and Visual Science Supplement*, 19(44A).

Perkins, M. E., & Landy, M. S. (1991). Nonadditivity of masking by narrow-band noises. *Vision Research*, 31, 1053–1065.

Press, W. H., Teukolsky, S. A., Vetterling, W. T., & Flannery, B. P. (1992). *Numerical recipes in C: the art of scientific computing*, 2nd. Cambridge: Cambridge University Press.

Rovamo, J., Franssila, R., & Nasanen, R. (1992). Contrast sensitivity as a function of spatial frequency, viewing distance and eccentricity with and without spatial noise. *Vision Research*, 32, 631–637.

Sachs, M. B., Nachmias, J., & Robson, J. G. (1971). Spatial frequency channels in human vision. *Journal of the Optical Society of America*, 61, 1176–1186.

Sankeralli, M. J., & Mullen, K. T. (1997). Postreceptoral chromatic detection mechanisms revealed by noise masking in three-dimensional cone contrast space. *Journal of the Optical Society of America A*, 14, 2633–2646.

Sharpe, C. T., & Tolhurst, D. J. (1973). Orientation and spatial frequency channels in peripheral vision. *Vision Research*, 13, 2103–2112.

Stromeyer III, C. F., & Julesz, B. (1972). Spatial frequency masking in vision: critical bands and spread of masking. *Journal of the Optical Society of America*, 62, 1221–1232.

Swanson, W. H., & Wilson, H. R. (1985). Eccentricity dependence of contrast matching and oblique masking. *Vision Research*, 25, 1285–1296.

Switkes, E., Bradley, A., & De Valois, K. K. (1988). Contrast dependence and mechanisms of masking interactions among chromatic and luminance gratings. *Journal of the Optical Society of America A*, 5, 1149–1162.

Watson, A. B. (1982). Summation of grating patches indicates many types of detector at one retinal location. *Vision Research*, 22, 17–25.

Watson, A. B. (1983). Detection and recognition of simple spatial forms. In O. J. Braddick, & A. C. Sleigh, *Physical and biological processing of images*. Berlin: Springer, 100–114.

Webster, M. A., De Valois, K. K., & Switkes, E. (1983). Orientation and spatial frequency discrimination for luminance and chromatic gratings. *Journal of the Optical Society of America A*, 7, 1034–1049.

Wilson, H. R., McFarlane, D. K., & Phillips, G. C. (1983). Spatial frequency tuning of orientation selective units estimated by oblique masking. *Vision Research*, 23, 873–882.

Wilson, H. R. (1991). Psychophysical models of spatial vision and hyperacuity. In D. Regan, & J. R. Cronly-Dillon, *Spatial vision*. In: *Vision and visual dysfunction*, Vol. 10. Boca Ratton: CRC Press, 64–86.